Available online at www.sciencedirect.com
SCIENCE DIRECT®

Journal of the European Ceramic Society 23 (2003) 153–159

www.elsevier.com/locate/jeurceramsoc

Quasistatic and dynamic properties of 1–3 composites made by soft molding

S. Gebhardt[a,*], A. Schönecker[a], R. Steinhausen[b], W. Seifert[b], H. Beige[b]

[a]*Fraunhofer-Institut für Keramische Technologien und Sinterwerkstoffe, Winterbergstr. 28, 01277 Dresden, Germany*
[b]*Martin-Luther-Universität Halle-Wittenberg, FB Physik, EP II, Friedemann-Bach-Platz 6, 06108 Halle/S., Germany*

Received 1 November 2001; received in revised form 4 March 2002; accepted 11 March 2002

Abstract

The development of the soft mold process allows for the preparation of fine scale 1–3 composites with PZT rods of different size, shape and spacing, which can be used as ultrasonic transducers for frequencies $\geqslant 5$ MHz. [Gebhardt, S., Schönecker, A., Steinhausen, R., Hauke, T., Seifert, W. & Beige, H., Fine scale 1-3 composites fabricated by the soft mold process: preparation and modeling. *Ferroelectrics*, 241 (2000) 67]. By this method, composites with a square, hexagonal and non regular arrangement of PZT rods of different shape have been fabricated and characterized by measuring their quasistatic and dynamic properties. The experimental results were compared with data from finite element method (FEM) modeling and analytical solutions. The vibrational characteristics of the composites were strongly influenced by the rod geometry and the rod arrangement. To evaluate the 1–3 composite performance, modal analysis and modeling of the impedance spectrum were carried out using the FEM package ANSYS.

Keywords: Composites; Dielectric properties; Finite element analysis; Piezoelectric properties; PZT

1. Introduction

1–3 composites consist of piezoelectric rods or fibers in a passive polymer matrix. Due to their low acoustic impedance, low mechanical quality and their high electromechanical coupling coefficient, they are well suited for ultrasonic transducers in non destructive testing and medical imaging applications. The standard commercial method to fabricate such composites remains the dice-and-fill method. Here, parallel and perpendicular cuts are made into a sintered and poled piezoceramic block, which are then backfilled with a polymer. The base is removed by grinding. This process is very laborious and time-consuming and thus, several alternative techniques have been developed to overcome these drawbacks.[3,4] As most of them are either expensive or restricted to certain rod geometries, they were not utilized at an industrial level.

Recently, we introduced the so-called soft mold process.[1,2] This method allows for a cost effective fabrication of piezocomposites, with rods of different size, shape and spacing. To evaluate the influence of rod geometry and arrangement on the transducer performance, composites with different volume fractions of square or cylindrical rods have been prepared and their quasistatic and dynamic properties have been measured. The experimental results have been compared to analytical solutions and finite element modeling. Special attention has been given to the vibrational characteristics of the 1–3 composites. Parasitic, lateral mode vibrations could be shifted, depending on the rod arrangement and inter pillar spacing. FEM was extended to simulate resonant modes and impedance curves of the piezocomposites.

2. Experimental procedure and basic modeling considerations

2.1. Composite preparation

The soft mold process uses master molds of arrayed rods, which have been structured by microsystems technology like micromachining, chemical or plasma etching. This allows designed shapes and arrangements of the ceramic elements. The transfer of the microstructured master mold, e.g. silicon (Si) master mold,

* Corresponding author. Tel.: +49-0351-2553-694; fax: +49-0351-2553-605.
E-mail address: sylvia.gebhardt@ikts.fhg.de (S. Gebhardt).

0955-2219/02/$ - see front matter
PII: S0955-2219(02)00077-8

into the ceramic mold is possible via a soft plastic template, which is reusable. The template, being the negative of the desired structure, is filled with a ceramic slurry. After drying, the ceramic green body can be demolded without defects and is subsequently sintered. A more detailed description of the process is given in.[1,2]

A powder of soft lead zirconate titanate (PZT) composition (PIC 151, PI Ceramic GmbH, Germany) was used. Samples of arrayed PZT rods with square and cylindrical geometry have been prepared successfully. For the squared rods a square arrangement and for the cylindrical rods a hexagonal arrangement was chosen, respectively. Also, one composite was prepared with a non regular arrangement of cylindrical rods of two different sizes. Examples of sintered PZT array structures are shown in Figs. 1–3.

The rod diameters were varied between 35 and 145 μm. The resultant aspect ratios of the rods (height:width) had a maximum of 6:1. The density was 97–98% of the theoretical. The arrays were then filled with an epoxy resin (Araldit 2020, Ciba Spezialitätenchemie GmbH, Germany) and the base was removed by grinding. The 1–3 composites were subsequently electroded by sputtering on gold. Poling was done in oil at room temperature with 2.2 kV/mm for 30 min. Samples, which were characterized are listed in Table 1.

Si master molds for samples A and B have been prepared by dicing using a precision wafer saw. All other samples were made from Si master molds, which were structured by a deep reactive ion etching process (ASE™). The ASE™ process enables the production of fine scale structures of almost every geometry.

For comparison, a bulk ceramic sample was prepared under same conditions.

2.2. Measurement equipment

The measurement of dielectric and electromechanical properties was done at least 24 h after poling. In the following, the piezocomposite material properties are indicated by a subscript index eff (effective).

The capacitance (C) was measured at 1 kHz, using a Hewlett Packard 4194A impedance analyzer to determine the relative dielectric constant of the composites $\varepsilon^{T}_{33,\mathrm{eff}}/\varepsilon_0$. The measurement of the piezoelectric coefficient of the composites $d_{33,\mathrm{eff}}$ was carried out at 130 Hz, using an equipment based on a capacitive detector.[5] Here, a variation in thickness of the sample by applying an alternating field causes a change of capacity of an air gap capacitor, which is part of a high frequency (HF) resonance circuit. This results in a frequency modulation of the HF circuit, which is compensated by a quartz crystal, connected mechanically in series with the sample. After demodulation, a voltage proportional to the strain of the sample is obtained.

The thickness mode coupling coefficient $k_{\mathrm{t,eff}}$ has been calculated from minimum (f_{min}) and maximum (f_{max})

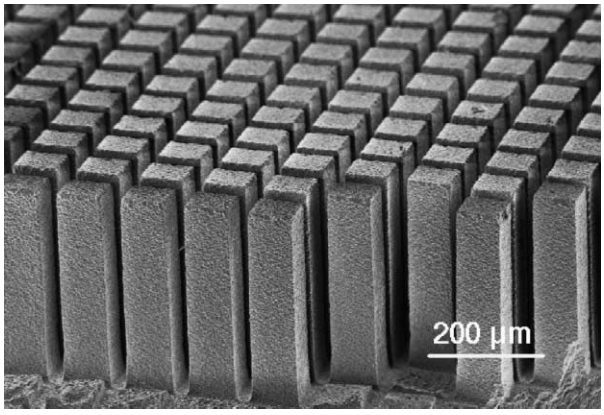

Fig. 1. SEM micrograph of a PZT array structure with square rods in a square arrangement (sample A—rod edge: 81 μm, inter pillar spacing: 36 μm, rod height: 309 μm).

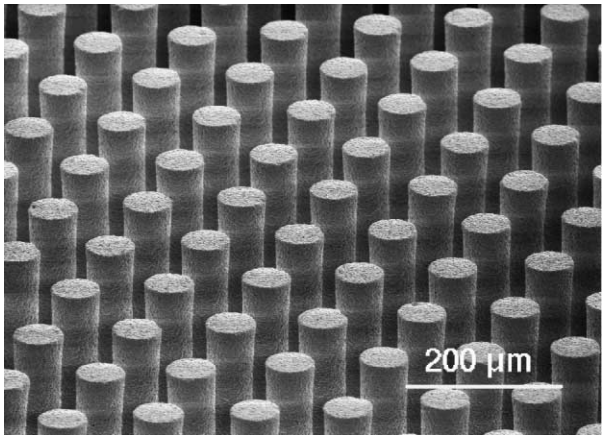

Fig. 2. SEM micrograph of a PZT array structure with cylindrical rods in a hexagonal arrangement (sample G—rod diameter: 65 μm, inter pillar spacing: 62 μm, rod height: 309 μm).

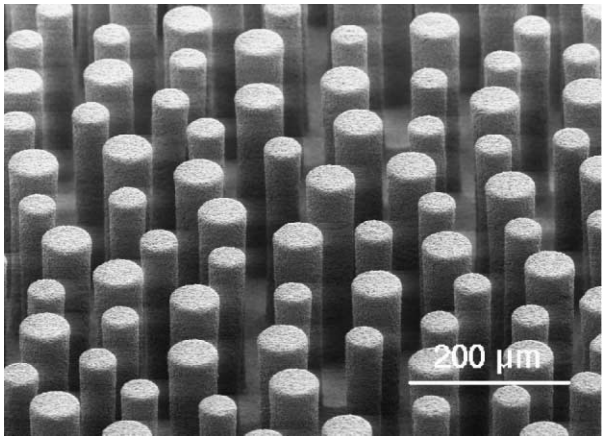

Fig. 3. SEM micrograph of a PZT array structure with cylindrical rods in a non regular arrangement (sample I—rod diameter: 65 and 48 μm, inter pillar spacing: non regular, rod height: 325 μm).

Table 1
Geometrical properties of characterized 1–3 composites

Sample	Rod shape	Rod arrangement	Master mold preparation	Rod edge/diameter (μm)	Inter pillar spacing (μm)	PZT content (vol.%)
A	Square	Square	dicing	81	36	48
B	Square	Square	dicing	145	45	58
C	Square	Square	ASE™	65	79	20
D	Square	Square	ASE™	65	62	26
E	Square	Square	ASE™	65	43	36
F	Cylindrical	Hexagonal	ASE™	65	79	18
G	Cylindrical	Hexagonal	ASE™	65	62	24
H	Cylindrical	Hexagonal	ASE™	65	43	33
I	Cylindrical	Non regular	ASE™	65, 48	> 43	22

frequency of impedance curve, recorded by an Hewlett Packard 4194A impedance analyzer using of the following equation:

$$k_{t,\mathrm{eff}}^2 = \frac{\pi}{2}\frac{f_{\min}}{f_{\max}}\tan\left(\frac{\pi}{2}\frac{f_{\max}-f_{\min}}{f_{\max}}\right) \quad (1)$$

The acoustic impedance $Z_{a,\mathrm{eff}}$ is given by:

$$Z_{a,\mathrm{eff}} = 2\rho_{\mathrm{eff}} t f_{\max} \quad (2)$$

where t is the thickness and ρ_{eff} the density of the piezocomposites. The density was determined from sample dimension and weight.

The elastic stiffness $c_{33,\mathrm{eff}}^D$ of the composites is defined by the following equation:

$$c_{33,\mathrm{eff}}^D = 4t^2 f_{\max}^2 \rho_{\mathrm{eff}} \quad (3)$$

The combination of Eqs. (1) and (3) results in the elastic stiffness $c_{33,\mathrm{eff}}^E$:

$$c_{33,\mathrm{eff}}^E = \left(1 - k_{t,\mathrm{eff}}^2\right) c_{33,\mathrm{eff}}^D \quad (4)$$

2.3. Basic modeling considerations

Analytical approximations derived by [6,7] and FEM modeling were applied to predict the composite material parameters. The data set of the PZT material ($\varepsilon_{33}^T/\varepsilon_0 = 2109$, $s_{33}^E = 1.9\times10^{-11}$ m^2/N and $d_{33} = 423$ pC/N) was given from the powder supplier. Youngs modulus $Y = 3.89$ GPa and Poissons ratio $\nu = 0.38$ of the polymer were determined by sound velocity measurements.[8]

The package ANSYS was used for the FEM modeling. For the periodic composite structures, two 3-dimensional unit cells were chosen, as shown in Fig. 4. Since the geometry was uniform with respect to the thickness direction, they had a height of half composite thickness. The surfaces $x = 0$, $y = 0$, $z = 0$ were symmetry planes. The electric boundary conditions (electrodes) were defined as nodes of the upper and lower unit cell surfaces.

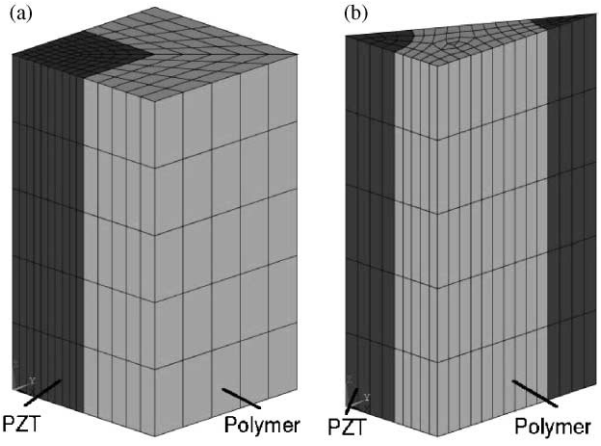

Fig. 4. Square (a) and hexagonal (b) unit cell for FEM modeling.

Static analysis was carried out to determine the quasistatic material properties $d_{33,\mathrm{eff}}$, $\varepsilon_{33,\mathrm{eff}}^T/\varepsilon_0$ and $c_{33,\mathrm{eff}}^E$. Therefore, displacements perpendicular to the surfaces were constrained to be identical for all surface nodes.

Eigenfrequencies and impedance curves were calculated with the modal and harmonic analysis of ANSYS, respectively. Since only frequencies in the vicinity of thickness mode resonance were of interest, the elastic boundary conditions were chosen so that the unit cell was laterally clamped. Thus, nodal motions perpendicular with respect to boundary planes, were inhibited.

For the harmonic analysis of ANSYS different damping mechanisms can be taken into consideration. We used specific damping constants for the ceramic and the polymer material, which resulted from fitting calculated with measured impedance curves.

3. Results and discussion

3.1. Quasistatic properties

Figs. 5 and 6 show the measured values of the piezoelectric coefficient $d_{33,\mathrm{eff}}$ and the dielectric constant

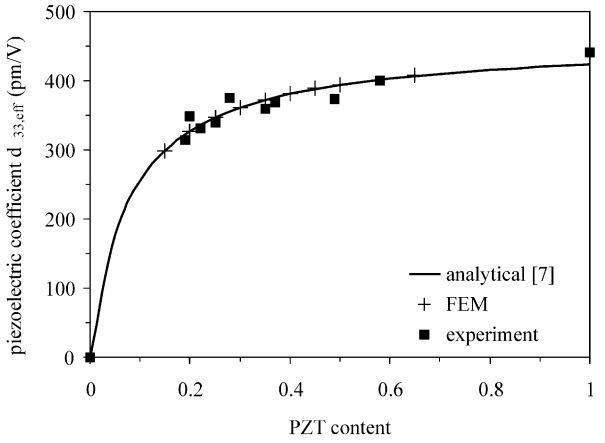

Fig. 5. Effective piezoelectric coefficient $d_{33,\mathrm{eff}}$ vs. PZT rod content: comparison between experimental results, analytical approximation (after [7]) and FEM modeling.

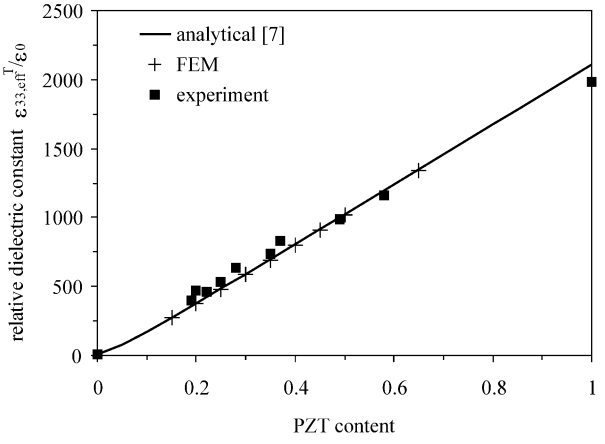

Fig. 6. Effective relative dielectric constant $\varepsilon^{T}_{33,\mathrm{eff}}/\varepsilon_0$ vs. PZT rod content: comparison between experimental results, analytical approximation (after [7]) and FEM modeling.

$\varepsilon^{T}_{33,\mathrm{eff}}/\varepsilon_0$ in comparison to data calculated by analytical approximations and FEM modeling.

In FEM modeling only a square unit cell was employed, because there is only an infinitely small influence of rod shape and arrangement on the composites quasistatic properties, as had been reported earlier.[9]

The analytical approximations were confirmed by FEM, and the experimental results are in a good correspondance to the calculated results.

3.2. Dynamic properties

The elastic stiffness $c^{E}_{33,\mathrm{eff}}$ was determined by the resonance frequency method [Eq. (4)]. The experimental results were verified by data obtained from analytical approximation and FEM modeling (Fig. 7).

In addition, the thickness mode coupling coefficient $k_{\mathrm{t,eff}}$ and acoustic impedance $Z_{\mathrm{a,eff}}$ showed the expected behavior (Figs. 8 and 9), although $k_{\mathrm{t,eff}}$ attained slightly lower values. The low $k_{\mathrm{t,eff}}$ is observed in samples with a

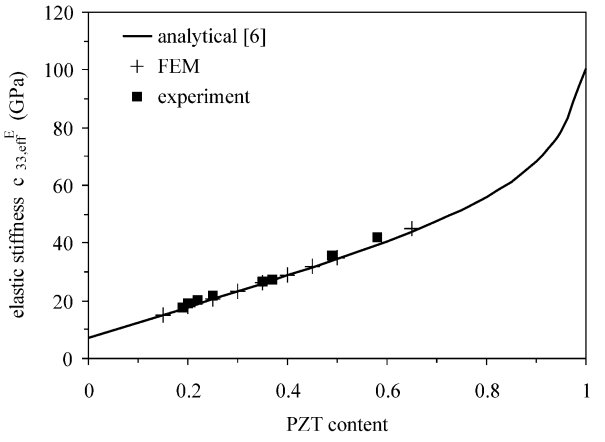

Fig. 7. Effective elastic stiffness $c^{E}_{33,\mathrm{eff}}$ vs. PZT rod content: comparison between experimental results, analytical approximation (after [6]) and FEM modeling.

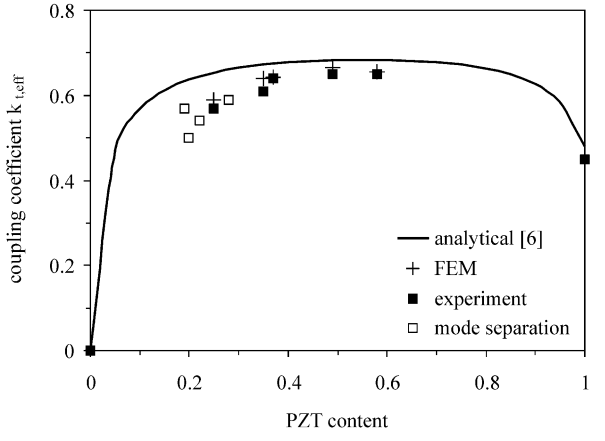

Fig. 8. Effective thickness mode coupling coefficient $k_{\mathrm{t,eff}}$ vs. PZT rod content: comparison between experimental results and analytical approximation (after [6]) and FEM modeling. Data represented by open symbols were calculated from separated thickness mode impedance curves.

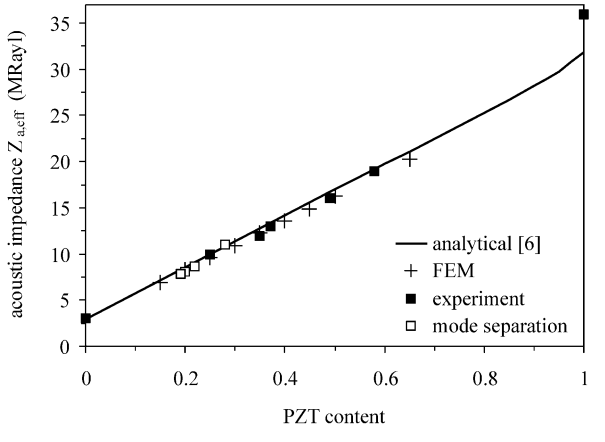

Fig. 9. Effective acoustic impedance $Z_{\mathrm{a,eff}}$ vs. PZT rod content: comparison between experimental results and analytical approximation (after [6]) and FEM modeling. Data represented by open symbols were calculated from separated thickness mode impedance curves.

low content of PZT rods, where experimental $k_{t,eff}$ values deviate from the model curve. Similar results were found by Hossack et al.[10,11] The deterioration of the electromechanical coupling coefficient is caused by an overlapping of the first lateral stopband resonance with the thickness mode resonance for these samples, as can be seen later. By means of FEM on 1–3 composites with square rods in a square arrangement the authors showed that with decreasing height:width of the rods the thickness mode coupling coefficient decreases. For a 1–3 composite with 20 vol.% PZT rods with an aspect ratio of 3:1, which is the case for sample C, $k_{t,eff}$ reaches only 88% of the maximum value. Taking that into consideration, sample C would have a $k_{t,eff}=0.57$ instead of 0.5 and would thus lie at the calculated curve by analytical approximation.

The measured values were also confirmed by calculating the $k_{t,eff}$ from FEM modeled impedance curves, which resulted from the harmonic analysis of ANSYS, as can be seen in Fig. 8.

For samples, where the first lateral stopband resonance was lying very close to the thickness mode resonance, the overlapping modes had to be seperated mathematically. From the extracted impedance curve of the thickness vibration, $k_{t,eff}$ and $Z_{a,eff}$ were calculated. Within the diagrams in Figs. 8 and 9 the properties of these samples are thus represented by open symbols.

The vibrational characteristics of the 1–3 composites were described by measuring electrical impedance curves. They are presented in Fig. 10. The frequency resonance peaks can be classified into the main categories:

1. planar mode resonances f_s of the composite as a whole,
2. thickness mode resonance f_t and its third harmonic $3f_t$ of the composite,
3. lateral stopband resonances f_{t1} and f_{t2}, caused by the periodic arrangement of the rods within the composite.

An allocation of the resonance modes to frequencies, which were found in the measured impedance curves, was done, using modal analysis of ANSYS. This tech-

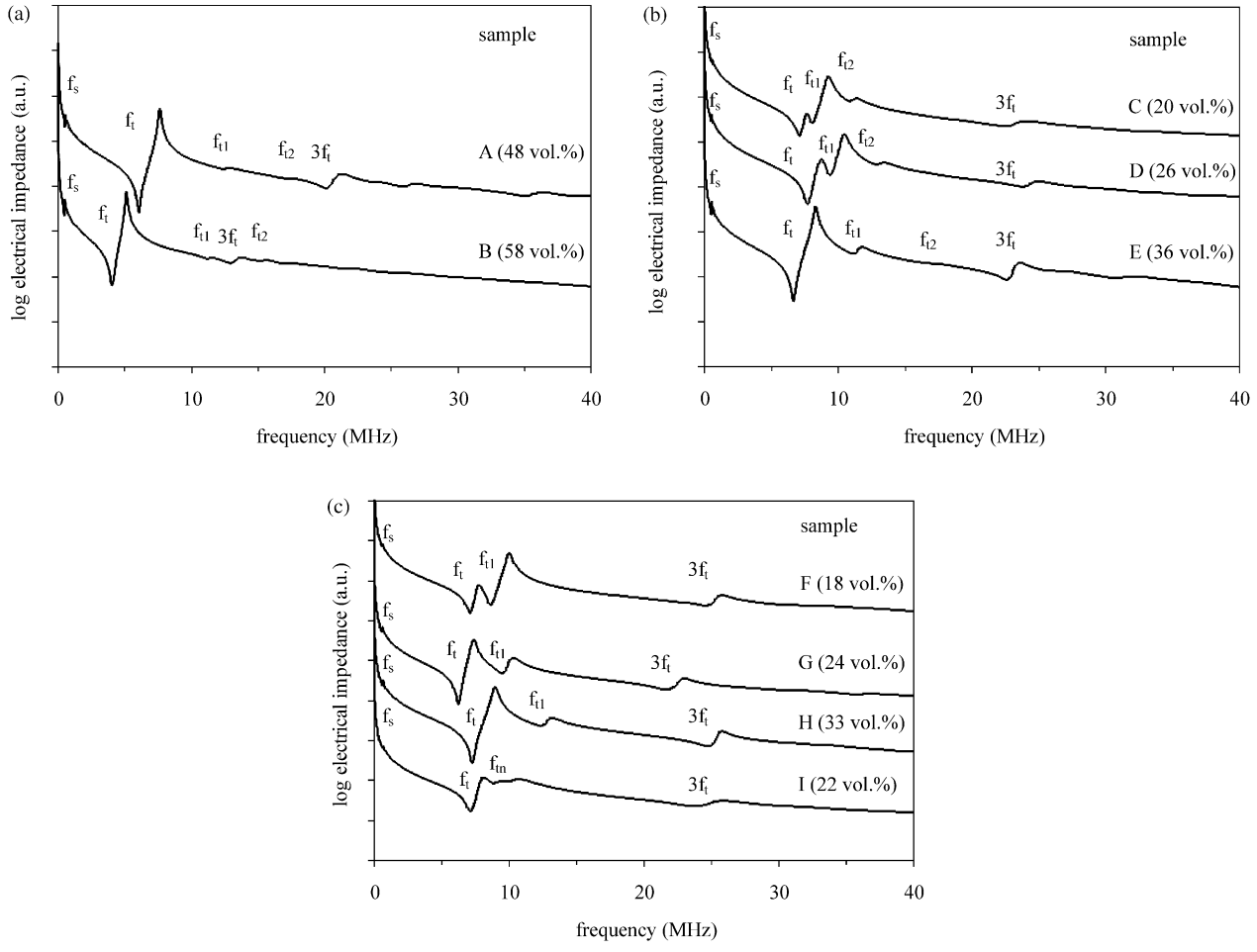

Fig. 10. Electrical impedance curves of 1–3 composites with (a) square rods in square arrangement (Si master molds structured by dicing), (b) square rods in square arrangement (Si master molds structured by ASE^{TM}) and (c) cylindrical rods in hexagonal (samples F, G, H) and unregular (sample I) arrangement (Si master molds structured by ASE™).

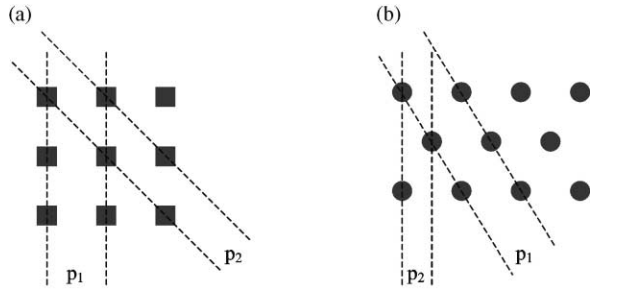

Fig. 11. Lateral stopband resonances caused by periodicities p_1 and p_2 within a square (a) and a hexagonal (b) unit cell.

nique neglects damping in the polymer and ceramic phase.

Piezocomposites with a square arrangement of square rods possessed two lateral stopband resonances f_{t1} and f_{t2}, according to periodicities p_1 and p_2 in Fig. 11a. For 1–3 composites with high aspect ratio PZT rods, these parasitic resonances were well separated from thickness mode resonance f_t. But, for sample C and D first lateral stopband resonance f_{t1} was in the vicinity of thickness mode resonance so that a complex vibration occurred (Fig. 10b).

The 1–3 composites with a hexagonal arrangement of cylindrical rods showed only one lateral stopband resonance f_{t1} (Fig. 10c), although modal analysis of ANSYS had shown that a second lateral stopband resonance corresponding to p_2 in Fig. 11b, should be excited too.

The reason for the suppression of this mode can be seen in the damping of the real polymer/PZT composite. By means of the harmonic analysis of ANSYS, which takes the mechanical damping of the composite components into consideration, the impedance curves could be modeled. Thus, not only the resonance frequencies, but also the amplitude of the electrical impedance could be calculated. In Fig. 12a and b modeled impedance curves of sample C (square arrangement) and sample F (hexagonal arrangement) are compared to measured values.

A comparison of 1–3 composites with a square arrangement of PZT rods to 1–3 composites with a hexagonal arrangement of PZT rods shows that by the same volume fraction the lateral stopband resonances can be shifted to higher frequencies. Therefore, 1–3 composites with a hexagonal structure or with an irregular structure should be prefered in future.

Surprisingly, sample I, which had an irregular arrangement of the rods, possessed parasitic modes (Fig. 10c), too. However, they were not as strong as for composites with a regular structure. An explanation for these lateral modes can be given considering the rod arrangement. Because inter pillar spacing could not be altered completely freely for technological reasons (tensile strength of the master mold and the soft plastic

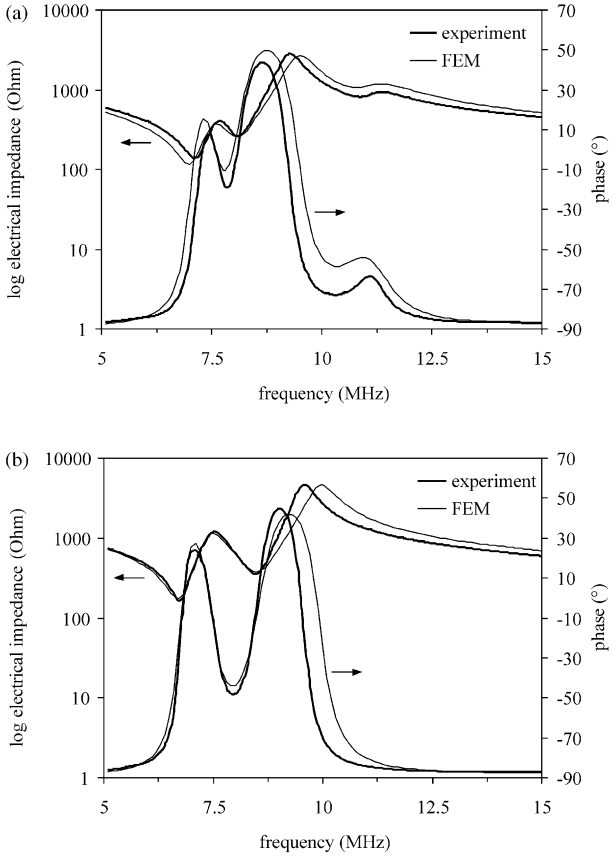

Fig. 12. Measured and FEM calculated impedance curves of a 1–3 composite with (a) square rods in square arrangement (sample C) and (b) cylindrical rods in hexagonal arrangement (sample F).

template), the rods were not arranged in a completely irregular manner. An evaluation of optical micrographs of the cross-section of sample I showed a concentration of rod center-to-center distances at 100–120 μm.

Because FEM could be extended to model resonance modes and impedance spectra of any unit cell, it should be possible in the future to design composite structures where the lateral stopband resonances are completely suppressed.

4. Conclusion

Fine scale 1–3 composites with variable rod shape, size and arrangement could be manufactured successfully, using the soft mold process. The starting point for this method were Si master molds which had been structured by dicing with a precision wafer saw or by anisotropic etching (ASE^{TM}). The transfer of the Si master mold into the ceramic structure was possible via soft plastic templates. Composites with square rods in a square arrangement and cylindrical rods in a hexagonal and non regular arrangement have been prepared and characterized.

The quasistatic and dynamic properties of the 1–3 composites are in excellent agreement with calculated data from analytical approximations and FEM modeling. Thus, ultrasonic transducers can be conceived and fabricated for specific applications on basis of the material parameters of the constituent components. FEM modeling can be used as a tool to develop structures which do not indicate lateral stopband resonance modes.

Acknowledgements

This work was supported by the Deutsche Forschungsgemeinschaft.

References

1. Starke, S., Schönecker, A. and Gebhardt, W., Fine scale piezoelectric 1–3 composites: a new approach of cost effective fabrication. In *Proceedings of the 11th IEEE International Symposium on Applications of Ferroelectrics*, ed. E. Colla, D. Damjanovic and N. Setter. The Institute of Electrical and Electronic Engineers, Inc, New York, 1998, pp. 393–396.
2. Gebhardt, S., Schönecker, A., Steinhausen, R., Hauke, T., Seifert, W. and Beige, H., Fine scale 1–3 composites fabricated by the soft mold process: preparation and modeling. *Ferroelectrics*, 2000, **241**, 67–73.
3. Safari, A., Janas, V. F. and Bandyopadhyay, A., Development of fine-scale piezoelectric composites for transducers. *AIChE J.*, 1997, **43**(11A), 2849–2856.
4. Janas, V. F. and Safari, A., Overview of fine-scale piezoelectric ceramic/polymer composite processsing. *J. Am. Ceram. Soc.*, 1995, **78**(11), 2945–2955.
5. Sorge, G., Hauke, T. and Klee, M., Electromechanical properties of thin ferroelectric-$PbZr_{0.53}Ti_{0.47}O_3$-layers. *Ferroelectrics*, 1995, **163**, 77–88.
6. Smith, W. A. and Auld, A., Modeling 1–3 composite piezoelectrics: thickness-mode oscillation. *IEEE Transactions on Ultrasonics, Ferroelectrics, and Frequency Control*, 1991, **38**(1), 40–47.
7. Smith, W. A., Modeling 1–3 composite piezoelectrics: hydrostatic response. *IEEE Transactions on Ultrasonics, Ferroelectrics, and Frequency Control*, 1993, **40**(1), 41–49.
8. Rabe, U., Fraunhofer IZFP, Saarbrücken, Germany, private communication.
9. Steinhausen, R., Hauke, T., Seifert, W., Beige, H., Watzka, W., Seifert, S., Sporn, D., Starke, S. and Schönecker, A., Finescaled piezoelectric 1–3 composites: properties and modeling. *J. Eur. Ceram. Soc.*, 1999, **19**, 1289–1293.
10. Hossack, J. A. & Hayward, G., Assessment of different pillar geometries for 1–3 composite transducers using finite element analysis. In *Proceedings of the 1990 IEEE Ultrasonics Symposium*. The Institute of Electrical and Electronic Engineers, Inc., New York, 1990, pp. 389–392.
11. Hossack, J. A. and Hayward, G., Finite-element analysis of 1–3 composite transducers. *IEEE Transactions on Ultrasonics, Ferroelectrics, and Frequency Control*, 1991, **38**(6), 618–629.